Electronic Supplementary Material (ESI) for ChemComm.

Electronic Supplementary Information

Salts of the Two-Coordinate Homoleptic Manganese(I) Dialkyl Anion $[Mn\{C(SiMe_3)_3\}_2]^-$ with Quenched Orbital Magnetism

C.-Y. Lin,[a] J.C. Fettinger,[a] N. F. Chilton,[b] A. Formanuik,[b] F. Grandjean,[c] G. J. Long,[c] and P. P. Power.[a]

[a] Department of Chemistry, University of California, Davis, California 95616, United States.

[b] School of Chemistry, The University of Manchester, Manchester, M13 9PL, United Kingdom.

[c] Department of Chemistry, Missouri University of Science and Technology, University of Missouri, Rolla, Missouri 65409-0010, United States.

Table of contents:

1. General experimental procedures

General considerations

All reactions were performed with the use of modified Schlenk techniques with or in a Vacuum Atmospheres OMNI-Lab drybox. All solvents were dried over an alumina column, followed by storage over a potassium mirror, and were degassed (freeze-pump-thaw) prior to use. 15-crown-5 and 18-crown-6 were purchased from Sigma-Aldrich and used as received. $Mn\{C(SiMe_3)_3\}_2$ were prepared according to a literature procedure.[S1] UV-visible spectra were recorded as dilute THF solutions in 3.5 mL quartz cuvettes using an Olis spectrophotometer. Melting points were measured in glass capillaries sealed under N_2 by using a Mel-Temp II apparatus and are uncorrected.

Magnetic Measurements

The polycrystalline samples of **1** and **2** used for magnetic measurements were coated with eicosane and sealed under vacuum in 3 mm diameter quartz tubing. The purple color of both samples was retained throughout the sealing process, and the compounds are stable under vacuum in sealed quartz tubes. The sample magnetization was measured using a Quantum Design MPMSXL7 superconducting quantum interference magnetometer. The magnetic susceptibility of **1** was measured in a DC field of 0.01 T. For compound **2** a DC field of 0.05 T was used above 30 K, while the in-phase AC susceptibility was measured below 30 K with an oscillating field of 0.155 mT. There was no out-of-phase signal observed and therefore the in-phase AC susceptibility represents the true zero-field differential magnetic susceptibility of **2**. The results were corrected for the diamagnetism of the eicosane and that of the sample.

X-Ray Crystallography

Crystals of **1** and **2** were removed from a Schlenk flask under a stream of N_2 and immediately covered with a layer of hydrocarbon oil. A suitable crystal was selected, attached to a glass fiber on a copper pin, and quickly placed in the cold N_2 stream on the diffractometer. Data for compound **1** and **2** were collected at ca. 90 K on a Bruker APEX DUO diffractometer with

Mo Kα radiation (λ = 0.71073 Å). Absorption corrections were applied using the SADABS program.[S2] The crystal structures were solved by direct methods and refined by full matrix least-squares procedures in the SHELXTL suite of programs.[S3] All non-H atoms were refined anisotropically. All H atoms were placed at calculated positions and included in the refinement using a riding model. Molecular graphics were produced by using the Olex2 program.[S4]

2. Details of the Synthesis and Spectroscopic Data for 1 and 2

2.1 $[K_2(18\text{-crown-}6)_3][Mn\{C(SiMe_3)_3\}_2]_2$ (1)

To a Schlenk flask containing freshly prepared KC_8 (prepared by heating 0.0103 g K (0.263 mmol) and 0.0334 g of graphite (2.78 mmol) until the mixture became a golden color) and a glass-coated magnetic stir bar was added a Et_2O solution of 0.118 g of $Mn\{C(SiMe_3)_3\}_2$ (0.228 mmol) and 0.917 g of 18-crown-6 (0.347 mmol) with cooling in an dry-ice/acetone bath. After the addition the bath was removed and the solution was slowly brought to room temperature and stirred overnight. The pale yellow solution had become a dark purple/blue color. The stirrer was switched off and the solids were allowed to settle. The supernatant liquid was filtered using a filter cannula, and the dark purple/blue filtrate was concentrated to incipient crystallization. Storage at ca. -18 °C freezer overnight to afford large, X-ray quality purple crystals of $[K_2(18\text{-crown-}6)_3][Mn\{C(SiMe_3)_3\}_2]_2$ (**1**). Yield: 0.035 g (16.1 %). Calcd. for $C_{76}H_{180}K_2Mn_2O_{18}Si_{12}$: C, 47.85; H, 9.51 %. Found: C, 47.43; H, 9.63 %. Compound **1** decomposes and melts as a dark oil at 160 – 163 °C.UV-Vis (THF): λ_{max} (ε_M, $M^{-1}cm^{-1}$) 244 (8600), 288 (3500), 578 (4400), 1028 (70) and 1334 (70) nm.

2.2 $[K(15\text{-crown-}5)_2][Mn\{C(SiMe_3)_3\}_2]$ (2)

To a Schlenk flask containing freshly prepared KC_8 (prepared by heating 0.0071 g K (0.18 mmol) and 0.0288 g of graphite (2.40 mmol) until the mixture turned a golden color) and a glass-coated magnetic stir bar was added a Et_2O solution of 0.0876 g of $Mn\{C(SiMe_3)_3\}_2$

(0.169 mmol) and 0.0917 g of 15-crown-5 (0.347 mmol) with cooling in an dry-ice/acetone bath. After the addition the bath was removed and the solution was slowly brought to room temperature and stirred overnight during which time the pale yellow solution had become pale purple/blue with purple colored **2** and graphite precipitate. The solution was removed under dynamic vacuum and THF (*ca.* 5 mL) was added to redissolve **2**. The solids were allowed to settle and the supernatant solution was filtered using a filter cannula. The dark purple filtrate was layered with hexanes and was stored at room temperature overnight to afford large, X-ray quality dark purple crystals of $[K(15\text{-crown-}5)_2][Mn\{C(SiMe_3)_3\}_2]$. Yield: 0.0290 g (17.2 %). Calcd. for $C_{40}H_{94}KMnO_{10}Si_6$: C, 48.14; H, 9.50 %. Found: C, 49.01; H, 9.71 %. Compound **2** decomposes and melts as a dark oil at 194 – 196 °C. UV-Vis (THF): λ_{max} (ε_M, $M^{-1}cm^{-1}$) 244 (5300), 284 (1800), 578 (2700), 948 (100), 1028 (110) and 1326 (70) nm.

3. X-ray crystallographic data and collection parameters

Table S1. Crystal data and structure refinement for **1**.

Identification code	CYL078FMI	
Empirical formula	$C_{76}H_{180}K_2Mn_2O_{18}Si_{12}$	
Formula weight	1907.35 g/mol	
Temperature	90(2) K	
Wavelength	0.71073 Å	
Crystal system	Triclinic	
Space group	P –1	
Unit cell dimensions	*a* = 12.5416(7) Å	□□= 87.7850(10)°
	b = 16.0775(9) Å	□□= 85.0576(10)°
	c = 27.2358(15) Å	□ = 79.8209(10)°
Volume	5383.7(5) $Å^3$	
Z	2	
Density (calculated)	1.177 Mg/m^3	
Absorption coefficient	0.499 mm^{-1}	
F(000)	2072	
Crystal size	0.238 x 0.106 x 0.070 mm^3	
Crystal color and habit	Purple Rod	
Diffractometer	Bruker APEX-II CCD	
Theta range for data collection	0.751 to 27.502°.	
Index ranges	-16<=h<=16, -20<=k<=20, -35<=l<=35	
Reflections collected	49077	
Independent reflections	24703 [R(int) = 0.0629]	
Observed reflections (I > 2sigma(I))	15550	
Completeness to theta = 25.242°	100.0 %	
Absorption correction	Semi-empirical from equivalents	
Max. and min. transmission	0.9500 and 0.8201	
Solution method	SHELXS-97 (Sheldrick, 2008)	
Refinement method	SHELXL-2013 (Sheldrick, 2013) Full-matrix least-squares on F^2	
Data / restraints / parameters	24703 / 84 / 1147	
Goodness-of-fit on F^2	1.037	
Final R indices [I > 2sigma(I)]	R1 = 0.0546, wR2 = 0.1110	
R indices (all data)	R1 = 0.1033, wR2 = 0.1280	
Largest diff. peak and hole	1.630 and -1.534 e.$Å^{-3}$	

Table S2. Crystal data and structure refinement for **2**.

Identification code	CYL090FMI	
Empirical formula	$C_{40}H_{94}KMnO_{10}Si_6$	
Formula weight	997.73 g/mol	
Temperature	90(2) K	
Wavelength	0.71073 Å	
Crystal system	Monoclinic	
Space group	*I*2/*a*	
Unit cell dimensions	*a* = 18.4983(10) Å	□□= 90°
	b = 14.4287(8) Å	□□= 90.8210(10)°
	c = 21.2812(11) Å	□ = 90°
Volume	5679.5(5) $Å^3$	
Z	4	
Density (calculated)	1.167 Mg/m^3	
Absorption coefficient	0.477 mm^{-1}	
F(000)	2168	
Crystal size	0.317 x 0.244 x 0.136 mm^3	
Crystal color and habit	Violet Block	
Diffractometer	Bruker APEX-II CCD	
Theta range for data collection	1.705 to 29.998°	
Index ranges	-26<=h<=26, -20<=k<=20, -29<=l<=29	
Reflections collected	31846	
Independent reflections	8283 [R(int) = 0.0242]	
Observed reflections (I > 2sigma(I))	7160	
Completeness to theta = 25.242°	100.0 %	
Absorption correction	Semi-empirical from equivalents	
Max. and min. transmission	0.9208 and 0.8081	
Solution method	SHELXT (Sheldrick, 2013)	
Refinement method	SHELXL-2014/6 (Sheldrick, 2014) Full-matrix least-squares on F^2	
Data / restraints / parameters	8283 / 0 / 320	
Goodness-of-fit on F^2	1.040	
Final R indices [I>2sigma(I)]	R1 = 0.0284, wR2 = 0.0713	
R indices (all data)	R1 = 0.0351, wR2 = 0.0751	
Largest diff. peak and hole	0.802 and -0.348 $e.Å^{-3}$	

4. UV-Vis-NIR Spectrum at Different Concentrations

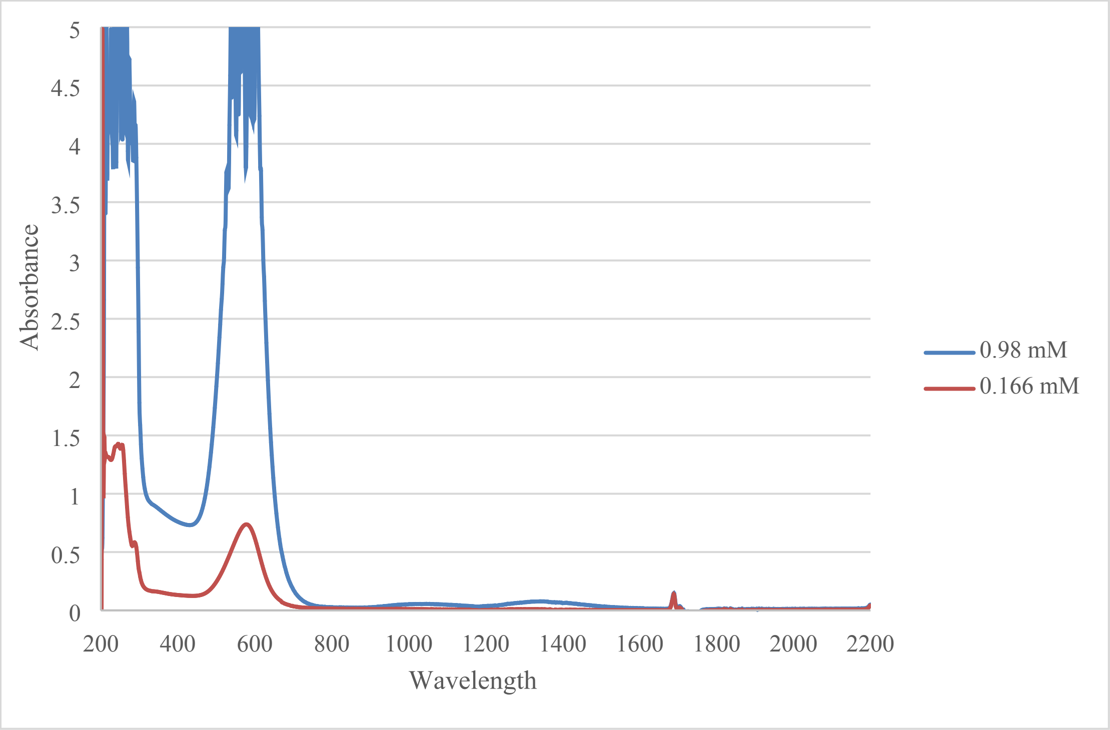

Figure S1. UV-Vis-NIR spectrum of $[K_2(18\text{-crown-}6)_3][Mn\{C(SiMe_3)_3\}_2]_2$ (**1**) in THF solution.

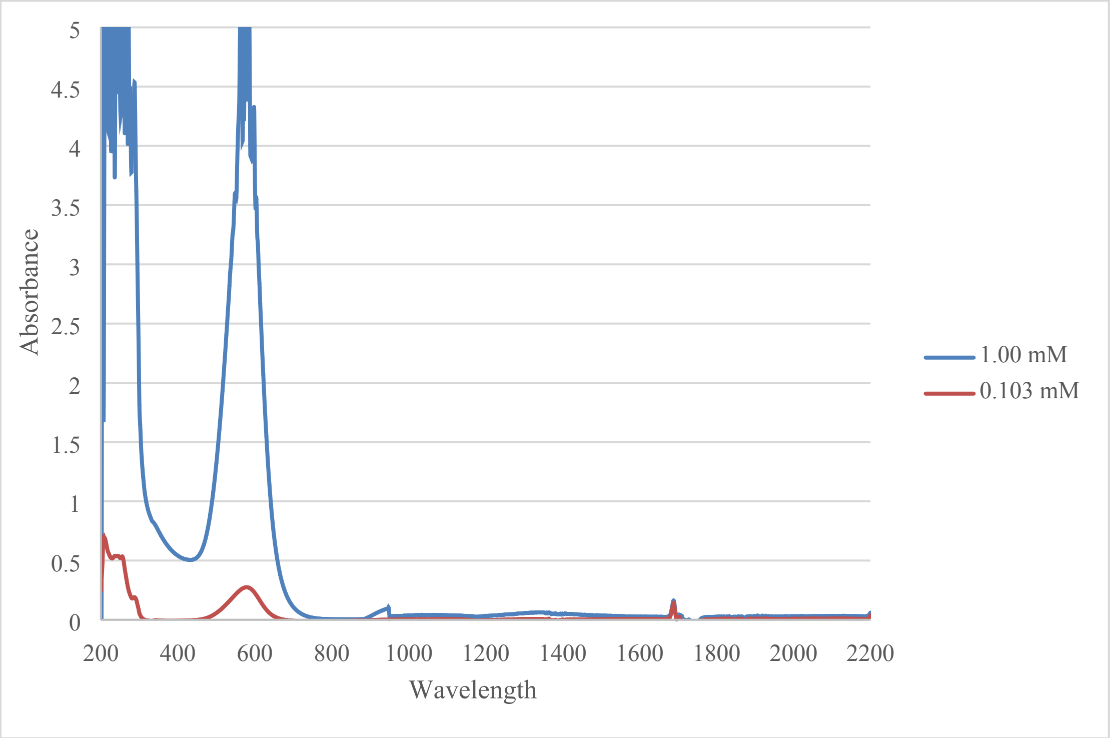

Figure S2. UV-Vis-NIR spectrum of $[K(15\text{-crown-}5)_2][Mn\{C(SiMe_3)_3\}_2]$ (**2**) in THF solution.

5. Computational approach

The CASSCF/RASSI/SINGLE_ANISO *ab initio* calculations have been performed with MOLCAS 8,[S5–S7] using the unoptimised X-ray structures of **1** and **2**. Basis sets from the MOLCAS ANO-RCC library[S8–S10] were utilized, with VTZP quality for the manganese(I) cation, VDZP quality for the carbon donors and VDZ quality for all the remaining atoms. The spin-orbit coupling was calculated with the atomic mean field integrals and the two-electron integrals were Cholesky decomposed. The active space in all cases was six electrons in five 3d orbitals. All five sextets, 45 triplets, and 50 singlets were included in the orbital optimisation and subsequently mixed by spin-orbit coupling. The SINGLE_ANISO routine[S11] was utilized to calculate the expectation of the $\hat{S}_z$ and $\hat{L}_z$ operators in the basis of pseudo-doublet states to determine the sign of D. The magnitude of D is easily determined from the gaps between the $S_z = \pm 2$, $S_z = \pm 1$ and $S_z = 0$ states, as $E(\pm2) - E(\pm1) = 3D$ and $E(\pm1) - E(0) = D$.

Table S3. Ground state $S = 2$ manifold for **1**:Mn(1). Subsequent excited states at 3954 cm^{-1}.

Energy (cm^{-1})	$\langle \hat{S}_z \rangle$	$\langle \hat{L}_z \rangle$
0.00	-	-
2.85	1.00	0.00
3.11		
11.88	2.00	0.00
11.88		

Table S4. Ground state $S = 2$ manifold for **1**:Mn(1B). Subsequent excited states at 2614 cm^{-1}.

Energy (cm^{-1})	$\langle \hat{S}_z \rangle$	$\langle \hat{L}_z \rangle$
0.00	2.00	0.20
0.04		
10.13	1.00	0.10
11.02		
14.12	-	-

Table S5. Ground state $S = 2$ manifold for **1**:Mn(2). Subsequent excited states at 4167 cm^{-1}.

Energy (cm^{-1})	$\langle \hat{S}_z \rangle$	$\langle \hat{L}_z \rangle$
0.00	-	-
2.58	1.00	0.00
3.21		
11.53	2.00	0.00
11.54		

Table S6. Ground state $S = 2$ manifold for **2**. Subsequent excited states at 4192 cm^{-1}.

Energy (cm^{-1})	$\langle \hat{S}_z \rangle$	$\langle \hat{L}_z \rangle$
0.00	-	-
2.56	1.00	0.00
3.24		
11.54	2.00	0.00
11.55		

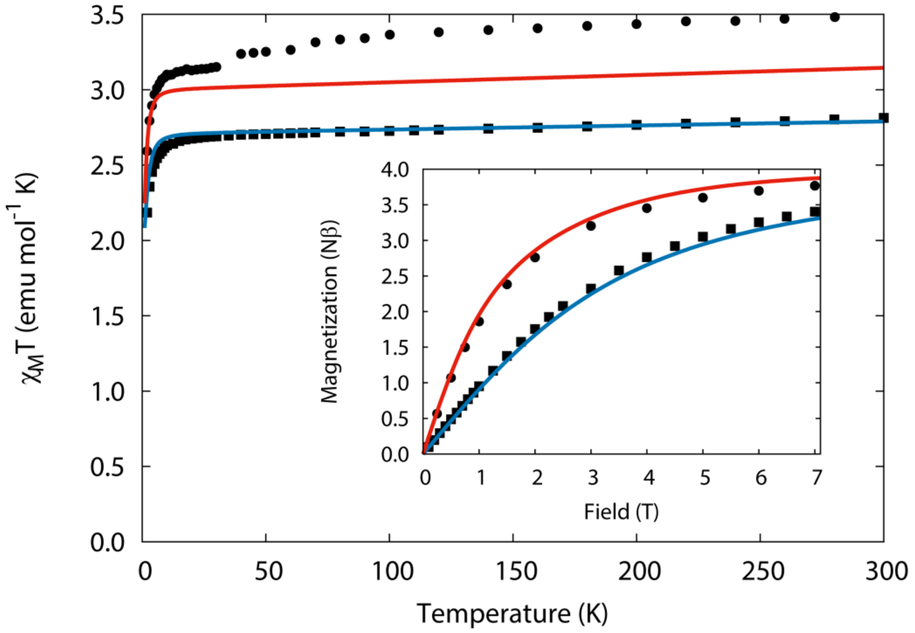

Figure S3. The experimental and fitted $\chi_M T$ product per Mn of **1** (black squares/blue line) and **2** (black circles/red line), and the 5 and 2 K magnetisation per Mn for **1** and **2**, respectively (inset). Fits are for $S = 2$ with the parameters given for D < 0 in Table 1 in the main text, cf. Figure 4 in the manuscript, which has parameters given for D > 0.

6. EPR spectroscopy

Crystalline samples of **1** and **2** were ground to a powder under an Ar atmosphere in a dry glove-box and loaded into quartz EPR tubes. For X- and K-band measurements, the tubes were evacuated and flame-sealed, while for W-band measurements the tubes were sealed with wax. In all cases the samples retained their purple colour and were therefore intact. X-band measurements were performed at 260 K with a Bruker EMX Micro spectrometer using an ER 4123SHQE Super-High Q resonator, operating at ~ 9.3 GHz between 0 and 0.8 T, Figures S4 and S5. K-band measurements were performed at 100 K with a Bruker Super-K CW bridge attached to an E580 console with an ER 6706KT resonator, operating at ~ 23.9 GHz between 0 and 1.4 T, Figures S6 and S7. W-band measurements were performed at room temperature with a Bruker E600 console and a W band resonator, operating at ~ 94 GHz between 0 and 6 T, Figures S8 and S9. Temperature dependence of the spectra were checked at X- and K-band, but no changes were observed. The spectra for both compounds show the same features, though slightly broader for **1** than for **2**, likely as a consequence of the presence of three crystallographically unique sites. The spectra for **2** have been fit with PHI using an $S = 5/2$ model ($g_{xy} = 1.9988$, $g_z = 2.0090$, $D = 0.22027$ cm^{-1}, $E = 0.054113$ cm^{-1}, isotropic Gaussian line widths of 1.0515 cm^{-1}, 1.0507 cm^{-1} and 0.69114 cm^{-1} for X-, K- and W-band, respectively); the spectra cannot be interpreted on the basis of an $S = 2$ model. As the magnetic data and CASSCF calculations unambiguously show that both compounds have an $S = 2$ ground state with a significant ZFS, we assign this EPR signal to that of a small $S = 5/2$ impurity (most likely Mn(II)) where the species of interest are EPR silent. At this stage the X-band signal at ~ 0.3 T cannot be accounted for, however as this is the $g = 2$ region the signal could be another small impurity.

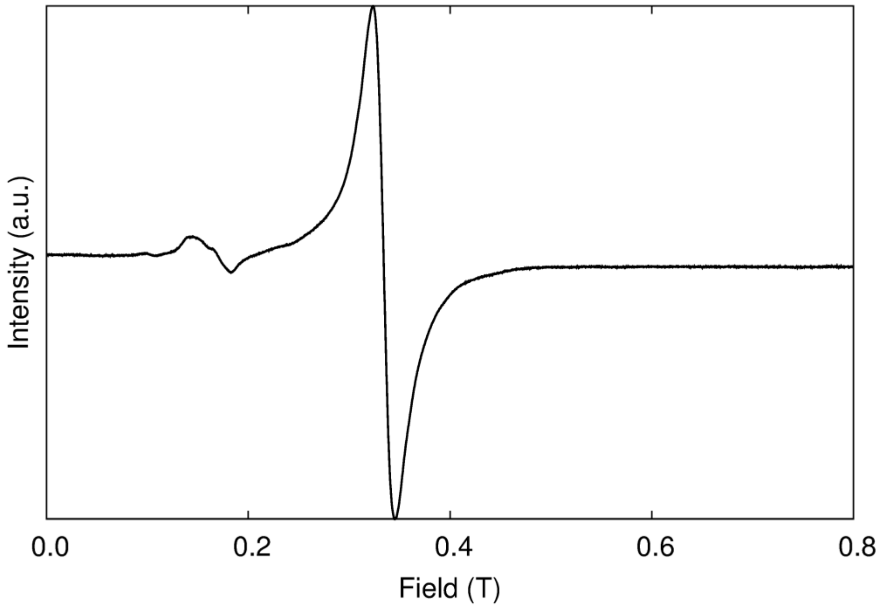

Figure S4. EPR spectrum of **1** at X-band (black line).

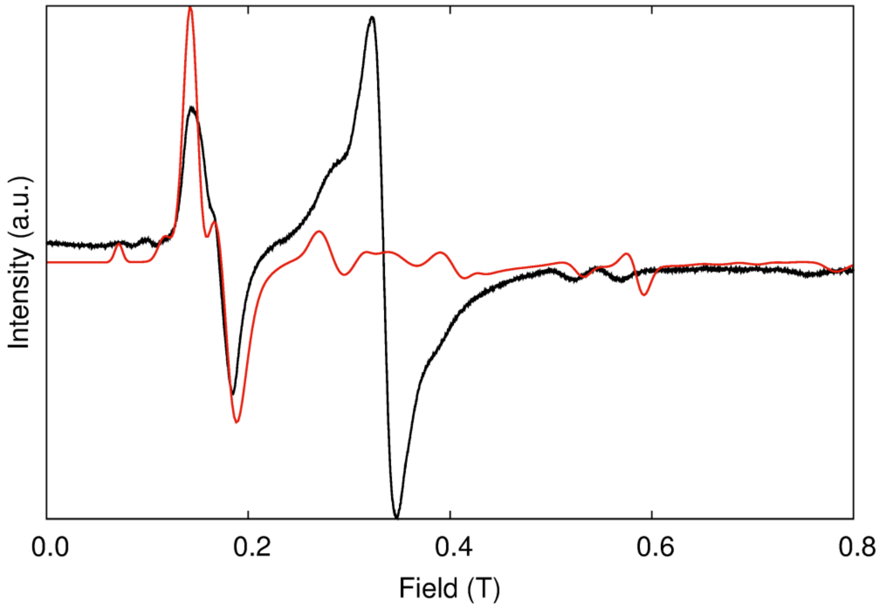

Figure S5. EPR spectrum of **2** at X-band (black line). Red line is a fit with parameters given in the text.

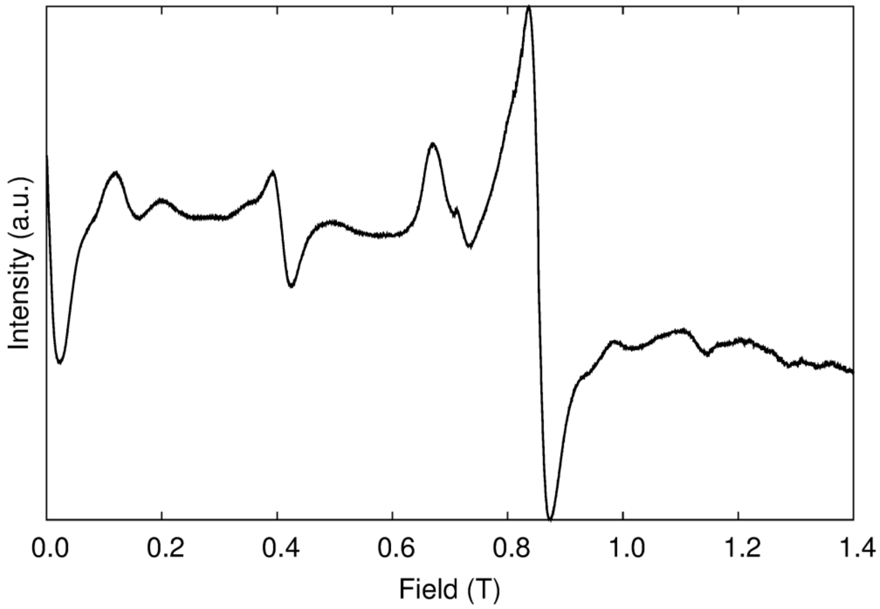

Figure S6. EPR spectrum of **1** at K-band (black line).

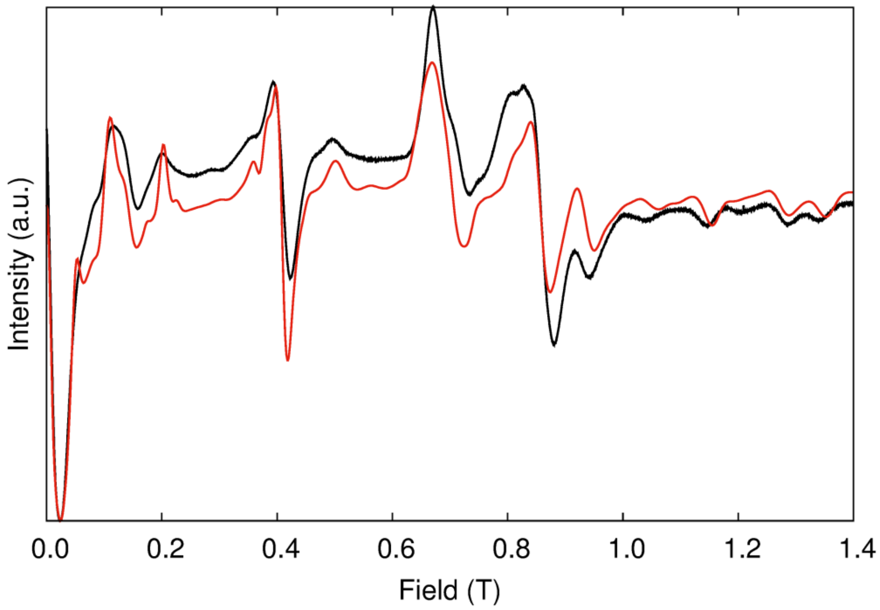

Figure S7. EPR spectrum of **2** at K-band (black line). Red line is a fit with parameters given in the text.

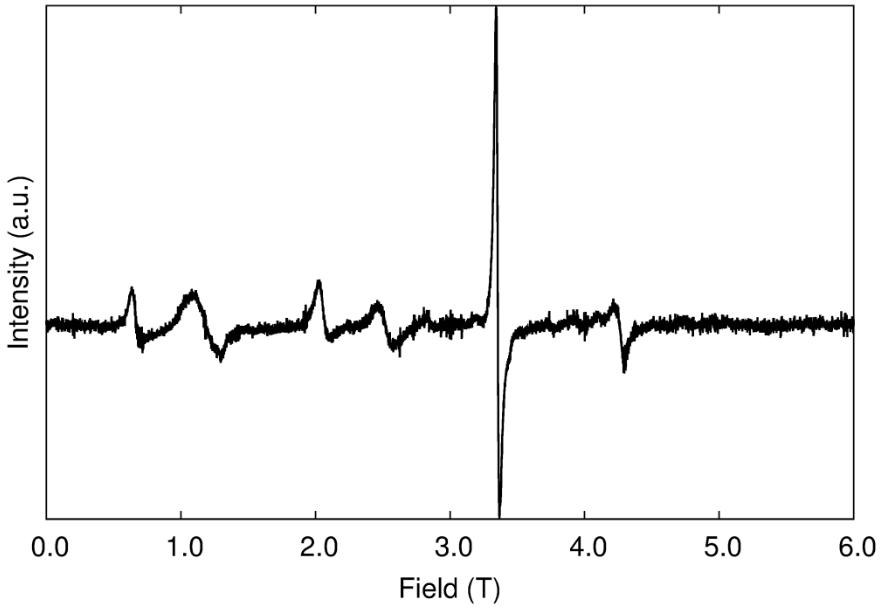

Figure S8. EPR spectrum of **1** at W-band (black line). The spectrum has been baseline corrected and the signals below ~ 2.2 T are artefacts of the cavity.

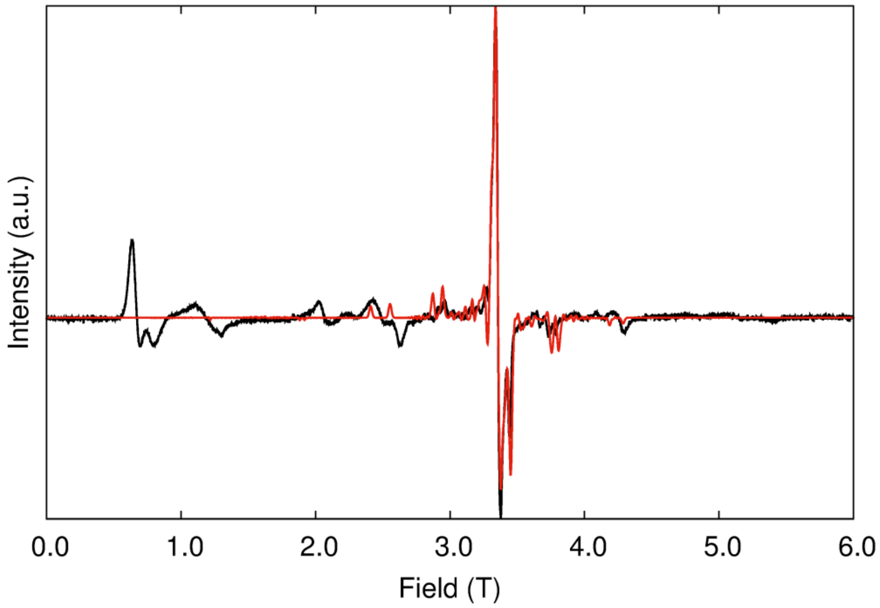

Figure S9. EPR spectrum of **2** at W-band (black line). Red line is a fit with parameters given in the text. The spectrum has been baseline corrected and signals below ~ 2.2 T are artefacts of the cavity.

7. References

S1. N. H. Buttrus, C. Eaborn, P. B. Hitchcock, J. D. Smith, and A. C. Sullivan, J. Chem. Soc., Chem. Commun. 1985, 1380.

S2. SADABS, an empirical absorption correction program for the SAINT-Plus-NT, version 5.0, Bruker AXS, Madison, WI, 1998.

S3. SHELXTL, version 5.1, Bruker AXS, Madison, WI, 1998.

S4. Dolomanov, O. V.; Bourhis, L. J.; Gildea, R. J.; Howard, J. A. K.; Puschmann, H. *J. Appl. Cryst.* **2009**, *42*, 339.

S5. G. Karlström, R. Lindh, P.-Å. Malmqvist, B. O. Roos, U. Ryde, V. Veryazov, P.-O. Widmark, M. Cossi, B. Schimmelpfennig, P. Neogrady and L. Seijo, *Comput. Mater. Sci.*, 2003, **28**, 222.

S6. V. Veryazov, P. Widmark, L. Serrano-Andrés, R. Lindh and B. O. Roos, *Int. J. Quantum Chem.*, 2004, **100**, 626.

S7. F. Aquilante, L. De Vico, N. Ferré, G. Ghigo, P. Malmqvist, P. Neogrády, T. B. Pedersen, M. Pitoňák, M. Reiher, B. O. Roos, L. Serrano-Andrés, M. Urban, V. Veryazov and R. Lindh, *J. Comput. Chem.*, 2010, **31**, 224.

S8. B. O. Roos, V. Veryazov and P.-O. Widmark, *Theor. Chem. Acc.*, 2004, **111**, 345.

S9. B. O. Roos, R. Lindh, P.-Å. Malmqvist, V. Veryazov and P.-O. Widmark, *J. Phys. Chem. A*, 2004, **108**, 2851.

S10. B. O. Roos, R. Lindh, P.-Å. Malmqvist, V. Veryazov and P.-O. Widmark, *J. Phys. Chem. A*, 2005, **109**, 6575.

S11. L. F. Chibotaru and L. Ungur, *J. Chem. Phys.*, 2012, **137**, 064112.